



Journal of Applied and Computational Mechanics



Research Paper

Numerical Investigation into the Effects of Orientation on Subcooled Flow Boiling Characteristics

Amal Igaadi^{ID}, Hicham El Mghari^{ID}, Rachid El Amraoui

Laboratory of Energy and Materials Engineering (LEME), Faculty of Sciences and Technologies (FST), Sultan Moulay Slimane University (SMSU), Beni Mellal, Morocco

Received August 26 2022; Revised October 05 2022; Accepted for publication October 18 2022.

Corresponding author: A. Igaadi (amal.igaadi@usms.ma)

© 2022 Published by Shahid Chamran University of Ahvaz

Abstract. The progress reached in the high heat flux systems has required the development of appropriate thermal management approaches for dissipating the high heat fluxes, especially for small-scale devices. One of the most advantageous thermal management techniques is the utilization of subcooled flow boiling. In this work, the subcooled flow boiling of FC-72 is numerically simulated in a minichannel using ANSYS Fluent to investigate the effects of system pressure and gravitational orientation on the subcooled flow boiling thermal transfer performances. Two different orientations (vertical downflow and vertical upflow) were examined in the same conditions of heat flux ($q = 191553 \text{ W/m}^2$), mass flux ($G = 836.64 \text{ kg/(m}^2\text{s)}$) and inlet temperature ($T_{in} = 304.54 \text{ K}$), and under three different system pressures (102000, 120000, and 209900 Pa). The present computational study has been validated and a good agreement with the experimental data was demonstrated. The predicted results demonstrate that the increase in system pressure improves the thermal performance of subcooled flow boiling by an average enhancement of 15.94%. In addition, the vertical upflow orientation is more advantageous than the downflow orientation due to the buoyancy force that moves the bubbles towards the flow direction and leads to less chaotic liquid-vapor interactions. An average enhancement of 1.65% in the heat transfer coefficient is reached in the upflow orientation compared to the downflow orientation for the higher system pressure of 209900 Pa.

Keywords: Subcooled flow boiling, upflow, downflow, heat transfer, pressure drop.

1. Introduction

With the remarkable development of miniaturization of technical devices in new engineering technologies such as pharmaceuticals, chemicals, petrochemicals, and electronic equipment, the increase in thermal heat density has become a critical issue because it reduces the performance, and security of these systems.

Currently, subcooled flow boiling in small channels, as presented in Fig. 1, represents an excellent and effective thermal management solution to eliminate the high heat fluxes of the miniature devices due to advantages including the utilization of latent heat transfer of working fluids, channel size and low variation in the fluid temperature, which reduces the refrigerant flow, and pumping power. However, the subcooled flow boiling heat transfer process is not fully understood since it depends on many parameters, such as the properties of the working fluid, heat flux, mass flux, channel diameter, and surface characteristics. Therefore, the evaluation of effects of these factors on the subcooled flow boiling mechanism in minichannels has been the subject of extensive studies reported in the literature [1–13]. For example, Liu et al. [7] studied the effects of heat flux, mass flux, vapor quality and saturation pressure on the flow boiling characteristics of three refrigerants (R600a, R227ea, and R245fa) in a vertical minichannel. They found that for all refrigerants tested, the heat transfer coefficient was significantly influenced by heat flux and saturation pressure, while the effects of mass flux and vapor quality were negligible. Anwar et al. [8] revealed that the dominating factor of the flow boiling characteristics of R152a and R134a in a vertical minichannel was the heat flux. The drying heat flux increased with the mass flux and the influence of system pressure was negligible. However, in the study of Belyaev et al. [9], where the effects of channel diameter, mass flux, pressure and inlet temperature on the heat transfer of R113 and RC318 in two small channels have been examined, the critical heat flux was enhanced at small channel diameter, with increasing mass flux and inlet subcooling, but decreased with increasing the reduced pressure. Furthermore, in the study by Charnay et al. [10], parametric analyses of the effects of heat flux, mass velocity, and saturation temperature on the local heat transfer coefficient of R-245fa flow boiling in a horizontal minichannel were conducted. It was determined that in an intermittent flow, the heat transfer coefficient is independent of vapor quality and mass velocity, while in an annular flow, the heat transfer coefficient increases with vapor quality and/or mass velocity. Also, Yan et al. [11] investigated the flow boiling heat transfer characteristics of R134a in small channels by focusing on the effects of heat fluxes, mass fluxes, and saturation temperatures. They found that the heat transfer coefficient improved with mass flux and saturation temperature. Therefore, we can conclude from all these studies mentioned above that the subcooled flow boiling characteristics have different behaviours depending on the factors involved.



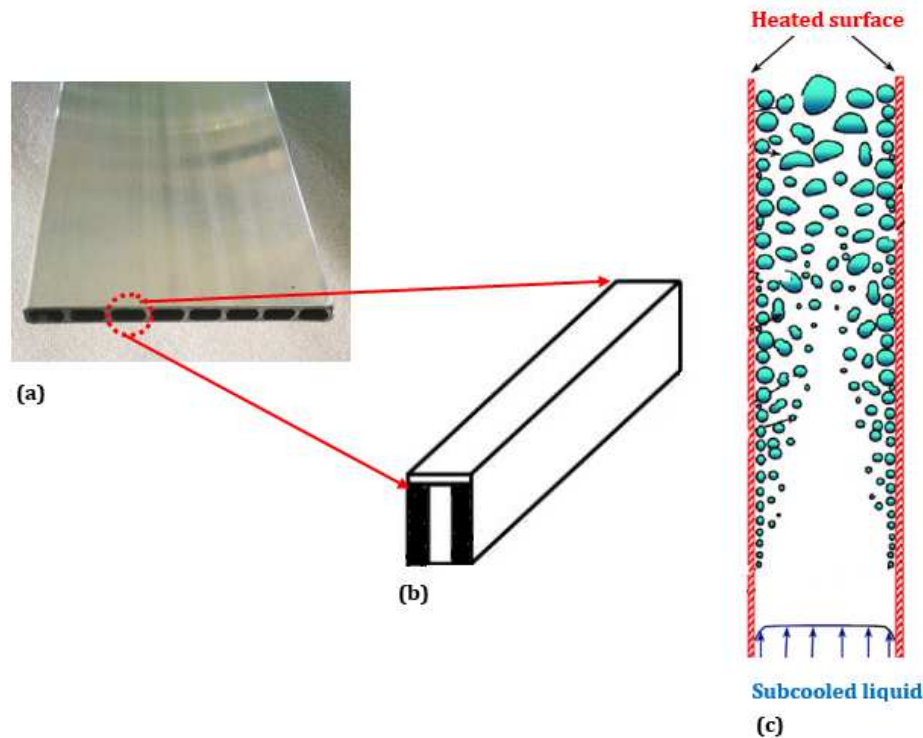


Fig. 1. (a) Cooling system based on the subcooled flow boiling in minichannels (b) schematic of single minichannel of the cooling system (c) schematic of x-y cross section of subcooled flow boiling in minichannel.

The minichannel in subcooled flow boiling can be placed horizontally, vertically, or at various angles according to the required operating conditions. Some previous studies reported in the literature [12-13] have neglected the effects of minichannel orientation on heat transfer performance, assuming that the surface force is the predominant force, even though gravity can exert different impacts due to the interaction between the buoyancy and the inertial forces. In fact, spatial orientation constitutes a crucial parameter that affects the subcooled boiling heat transfer characteristics. As Piasecka et al. [14] demonstrated, the vertical and inclined (45° to the horizontal plane) orientations resulted in higher heat transfer coefficients. Moreover, Vlachou et al. [15] discovered that inclinations of 60°, and 90° lead to a slight increase of 10% in the heat transfer coefficient compared to the horizontal case. Piasecka et al. [16] studied the flow boiling of FC-72, HFE-649, HFE-7000, and HFE-7100 in a minichannel in three spatial orientations (0°, 90°, and 180°). They reported that the highest heat transfer coefficient was obtained for the lowest heat flux at the horizontal position of 180°. Whereas, Sinha and Srivastava [17] studied the vapor bubble behaviour in subcooled flow boiling under vertical upward and downward flow. They found that greater evaporative heat flux dissipation was obtained for the upward flow for $Re \leq 6000$. Other studies [18-19] have investigated rotational orientation effects, such as Vermaak et al. [19], which studied the boiling of FC-72 flow in mini channels at different rotational orientations as a function of gravity. It was found that the bottom-heating cases (0° orientation) generated higher local heat transfer coefficients of up to 201% than for any other rotational orientation.

Although several research studies have concentrated on the subcooled flow boiling heat transfer in different spatial orientations, the detailed differences between the vertical upflow and downflow orientations of the subcooled flow boiling heat transfer and pressure drop characteristics have not been fully explained. For this reason, further research studies are needed to identify the key differences between subcooled flow boiling in vertical minichannel in upflow and downflow orientations.

Therefore, the purpose of the present work is to numerically investigate the effects of gravitational orientations and system pressure on the heat transfer characteristics and pressure drop of subcooled flow boiling of FC-72 in a vertical minichannel in both upflow and downflow orientations under three different system pressures from 102000 Pa to 209900 Pa.

2. Numerical Model

This paper performs two-dimensional numerical simulations of subcooled flow boiling in a minichannel in vertical upflow and downflow orientations under different system pressures. The following assumptions are made to simplify the present numerical model:

- Flow is Newtonian, unsteady, and turbulent;
- Liquid phase is incompressible;
- Vapour phase as an ideal gas;
- Thermo-physical properties of fluid and solid are constant at the corresponding system pressure.

2.1. Governing equations

This section outlines the details of the numerical model employed in our simulations. Thermophysical properties of FC-72 are also presented in Table 1. The volume of fluid (VOF) model is used for tracking the liquid-vapor interface during subcooled flow boiling by solving the conservation equations for both liquid and vapor phases and accounting for mass transfer between phases. The conservation equations are as follows:

For the liquid phase:

$$\frac{\partial}{\partial t}(\alpha_l \rho_l) + \nabla \cdot (\alpha_l \rho_l \vec{u}) = S_l \quad (1)$$



Table 1. Thermophysical properties of FC-72

	P = 102000 Pa		P = 120000 Pa		P = 209900 Pa	
FC-72 liquid	ρ_l (kg/m ³)	1570.3	ρ_l (kg/m ³)	1608.2	ρ_l (kg/m ³)	1622.9
	C_{pl} (J/kg.K)	1102	C_{pl} (J/kg.K)	1117.6	C_{pl} (J/kg.K)	1130.5
	k_l (W/m.K)	0.0524	k_l (W/m.K)	0.0536	k_l (W/m.K)	0.054
	μ_l (kg/m.s)	$3.846.10^{-4}$	μ_l (kg/m.s)	$4.09.10^{-4}$	μ_l (kg/m.s)	$4.24.10^{-4}$
FC-72 vapor	ρ_v (kg/m ³)	13.38	ρ_v (kg/m ³)	15.992	ρ_v (kg/m ³)	23.1
	C_{pv} (J/kg.K)	878	C_{pv} (J/kg.K)	942.87	C_{pv} (J/kg.K)	1259.8
	k_v (W/m.K)	0.013026	k_v (W/m.K)	0.0142	k_v (W/m.K)	0.015
	μ_v (kg/m.s)	$1.175.10^{-5}$	μ_v (kg/m.s)	$1.21.10^{-5}$	μ_v (kg/m.s)	$1.22.10^{-5}$

For the vapor phase:

$$\frac{\partial}{\partial t}(\alpha_v \rho_v) + \nabla \cdot (\alpha_v \rho_v \vec{u}) = S_v \quad (2)$$

where α_l and α_v are the volume fraction of the liquid phase and the vapour phase, respectively, ρ_l and ρ_v are the densities of the liquid and vapor phases, respectively, u is the drift velocity and S_l and S_v are the mass source terms due to phase change for the liquid and vapor phases, respectively.

The momentum and energy equations are applied to the combined phases and formulated as follows, respectively:

$$\frac{\partial}{\partial t}(\rho \vec{u}) + \nabla \cdot (\rho \vec{u} \vec{u}) = -\nabla P + \nabla \cdot [\mu(\nabla \vec{u} + (\nabla \vec{u})^T)] + \rho \vec{g} + \vec{F}_{csf} \quad (3)$$

$$\frac{\partial}{\partial t}(\rho E) + \nabla \cdot [\vec{u}(\rho E + P)] = \nabla \cdot (\lambda_{eff} \nabla T) + S_e \quad (4)$$

where P is the pressure, μ is the dynamic viscosity, g is the gravity acceleration, F_{csf} represents the surface tension force vector, E is the energy, T is the temperature, λ_{eff} is the thermal conductivity, and S_e is the energy source term. The surface tension effects across the liquid-vapor interface are taken into account by using the continuum surface force (CSF) model of Brackbill et al. [20].

$$\vec{F}_{csf} = 2\sigma \frac{\alpha_l \rho_l k_l \nabla \alpha_v + \alpha_v \rho_v k_v \nabla \alpha_l}{\rho_l + \rho_v} \quad (5)$$

where σ is the surface tension coefficient. k_l and k_v are the local interface curvatures of the liquid and vapor phases, respectively, which are determined by the gradient of the volume fraction scalar as:

$$k_l = \frac{\Delta \alpha_l}{|\nabla \alpha_l|} \quad (6)$$

$$k_v = \frac{\Delta \alpha_v}{|\nabla \alpha_v|} \quad (7)$$

The phase change Lee model [21] is adopted to define the mass and heat transfer rates. This model presumes a thermodynamic equilibrium at the liquid-vapor interface and depends on the saturation temperature (T_{sat}), as shown in the following expressions:

If $T_l < T_{sat}$ (evaporation):

$$S_l = \alpha_l \rho_l \frac{(T_l - T_{sat})}{T_{sat}} \quad (8)$$

If $T_l > T_{sat}$ (condensation):

$$S_v = \alpha_v \rho_v \frac{(T_v - T_{sat})}{T_{sat}} \quad (9)$$

Subsequently, the energy source (S_e) on the momentum equation (Eq. (3)) is available as follows:

$$S_e = h_{lv} S_l = h_{lv} S_v \quad (10)$$

2.2. Computational domain and boundary conditions

Figure 2 presents the details of the computational domain of the upflow and downflow subcooled flow boiling. The flow is along the y-axis, which represents the vertical direction. FC-72 is chosen as the working fluid, and copper is used as the solid material. In addition, the wall contact angle is fixed at 5°.

A constant mass flux boundary condition of 836.64 kg/(m²s) is applied at the inlet of the minichannel, and the subcooling of the entering FC-72 liquid is fixed at 30 K. Furthermore, at the outlet of the minichannel, the pressure boundary condition is applied, and the backflow temperature is fixed at 380 K. The boundary condition of uniform heat flux of 191553 W/m² is specified for the heated walls. Moreover, all the inner walls are considered as no-slip boundary conditions ($u_w = v_w = 0$).



Table 2. Numerical methods

Equation	Numerical method
Pressure-velocity coupling	PISO algorithm
Gradient	The green-gauss node-based method
Pressure	PRESTO
Momentum	Second order upwind scheme
Volume fraction	Geo-Reconstruct
Turbulent kinetic energy	First-order implicit scheme
Specific dissipation rate	First-order implicit scheme
Energy	Second order upwind scheme
Transient formulation	First-order implicit scheme

Table 2 presents different numerical procedures used to discretize the governing equations of the numerical model. The time step Δt is set to be variable in the range of 10^{-4} to 10^{-6} to keep the courant number (Co) less than 0.5, which helps to make the simulation more stable. Furthermore, we have considered that the convergence of the numerical solution is reached when the mass and velocity residuals are less than 10^{-4} and the temperature residual is below 10^{-6} .

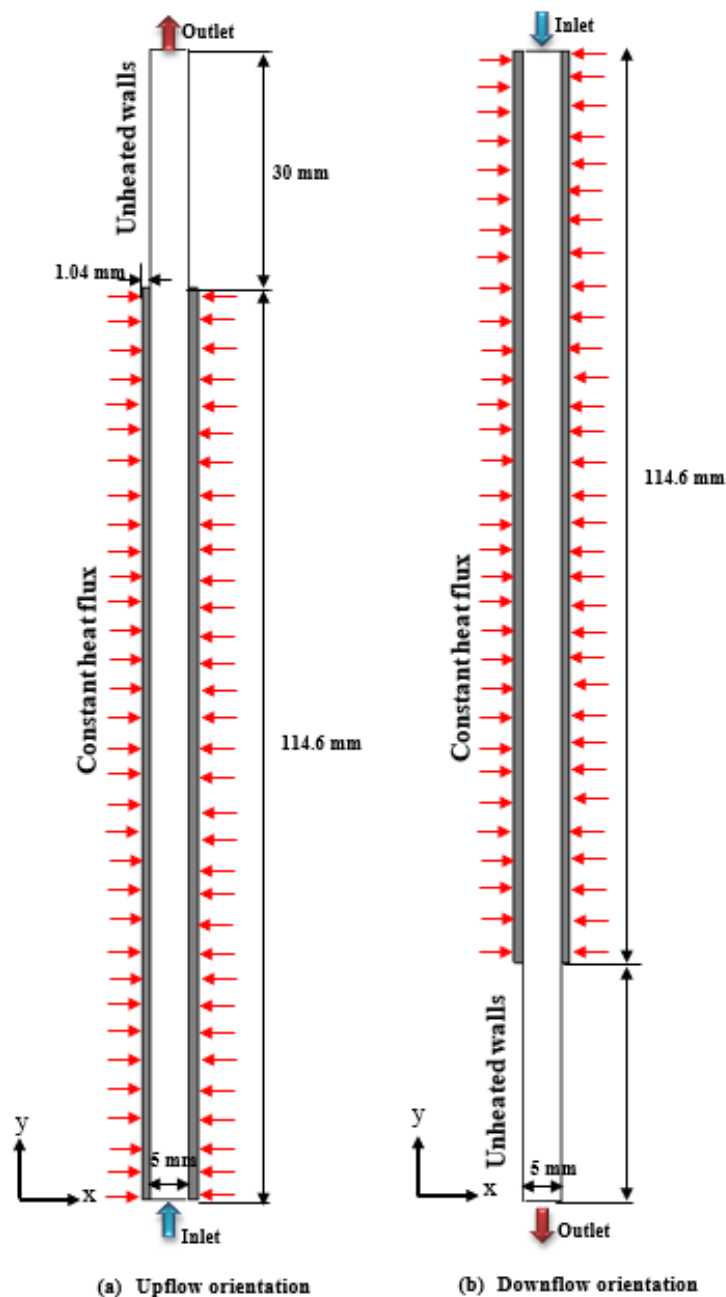


Fig. 2. Schematic of the computational domain.



2.3. Grid independence study

In this work, the quadrilateral mesh is used for all computational domains with a progressive refinement in the regions adjacent to the walls to precisely capture the formation of smaller bubbles. The mesh independence study was carried out. Therefore, five meshes with node numbers ranging from 33540 to 343760 are tested for the case where the system pressure was 120000 Pa, the mass flux was $836.64 \text{ kg}/(\text{m}^2\cdot\text{s})$, the heat flux was $191553 \text{ W}/\text{m}^2$, and the inlet temperature was 304.54 K.

Fig. 3 presents the variation of the area-weighted average temperature of walls over different grid numbers. It can be seen that, the area-weighted average wall temperature reduces as the number of nodes increases until the grid has 205495 nodes, i.e., independent of the mesh size. Therefore, the grid with 205495 nodes is chosen for all our simulations.

3. Validation

Validation of the current numerical model precision is established from the comparison of the present predictive results with the experimental results of Lee et al. [22] for the case where the system pressure was 120000 Pa.

As illustrated in Fig. 4, the average relative errors between the present numerical results of local heat transfer coefficients and experimental data are 18.097% and 20.687% for the left wall and right wall, respectively. This deviation from the experimental results could be related to the uncertainties and errors encountered in experimentation. In addition, Fig. 5 compared the experimental flow pattern visualization images with those predicted numerically. As can be seen, there is high accuracy in the prediction of bubble generation evolution. Therefore, this proves that the current computational model is both reasonable and effective.

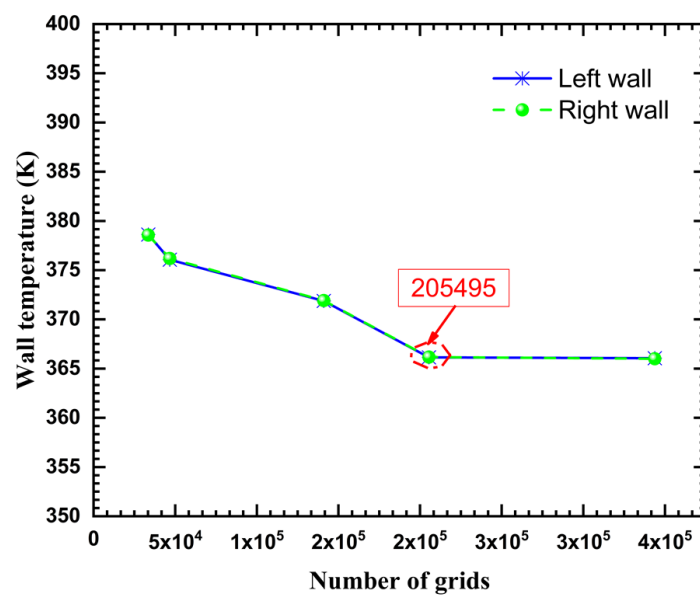


Fig. 3. Grid independency test results.

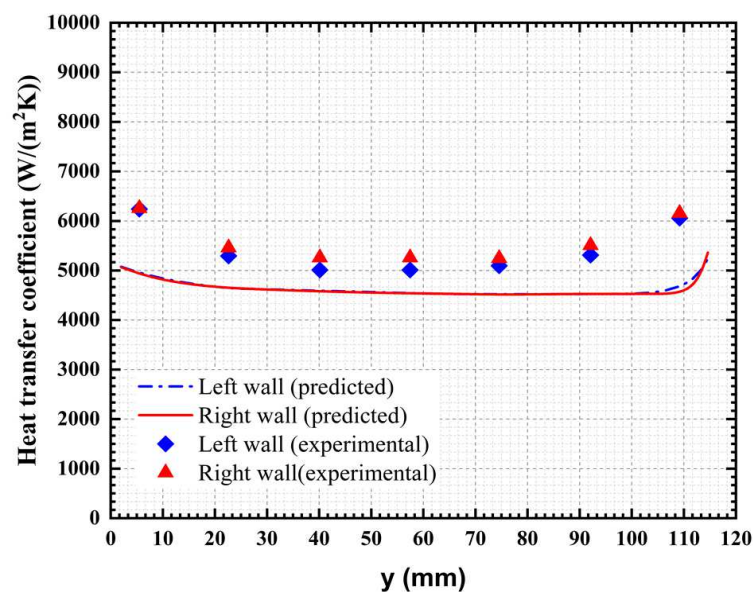


Fig. 4. Validation of the numerical model: comparison of the experimental heat transfer coefficient with those predicted numerically.



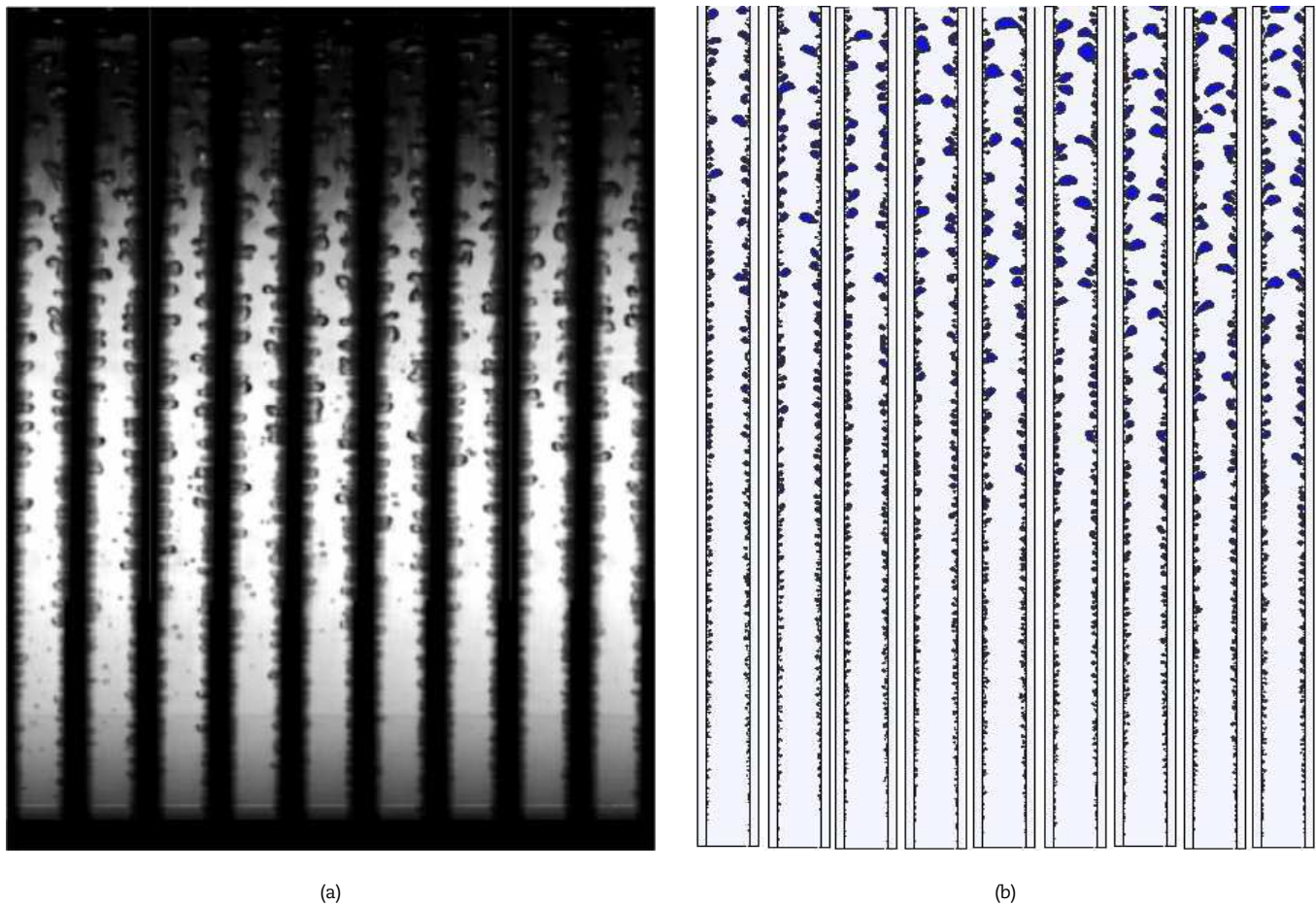


Fig. 5. Comparison of the (a) experimental data [22] and (b) simulation results in terms of flow patterns.

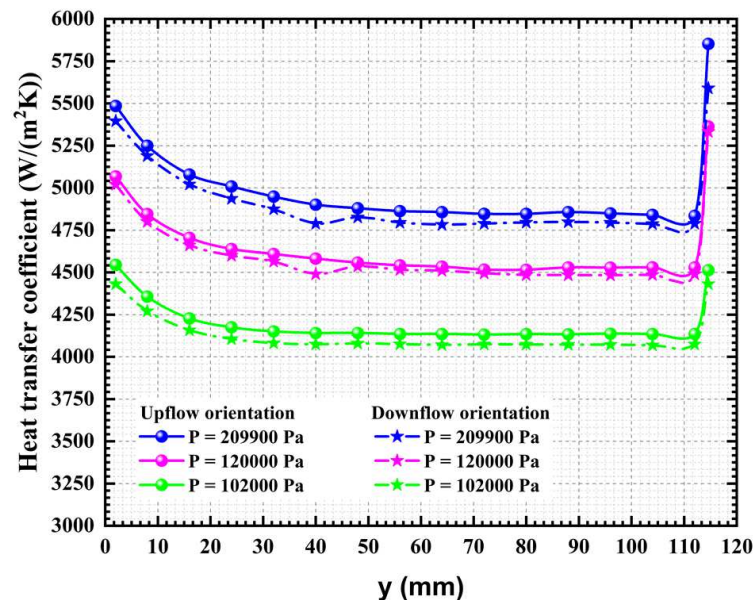


Fig. 6. Local heat transfer coefficient along the minichannel in the vertical upflow and downflow orientations for different system pressures.

4. Results

The effects of orientation and system pressure on the heat transfer characteristics of subcooled flow boiling in a minichannel are presented in Figs. 6 and 7. A mass flux of $836.64 \text{ kg/(m}^2\text{s)}$ is applied at the inlet, the subcooling of the entering liquid is fixed at 30 K , and the uniform heat flux of 191553 W/m^2 is applied to the heated walls. The system pressure varied from 102000 Pa to 209900 Pa , and the saturation temperature varied accordingly from 330.47 K to 348.15 K .



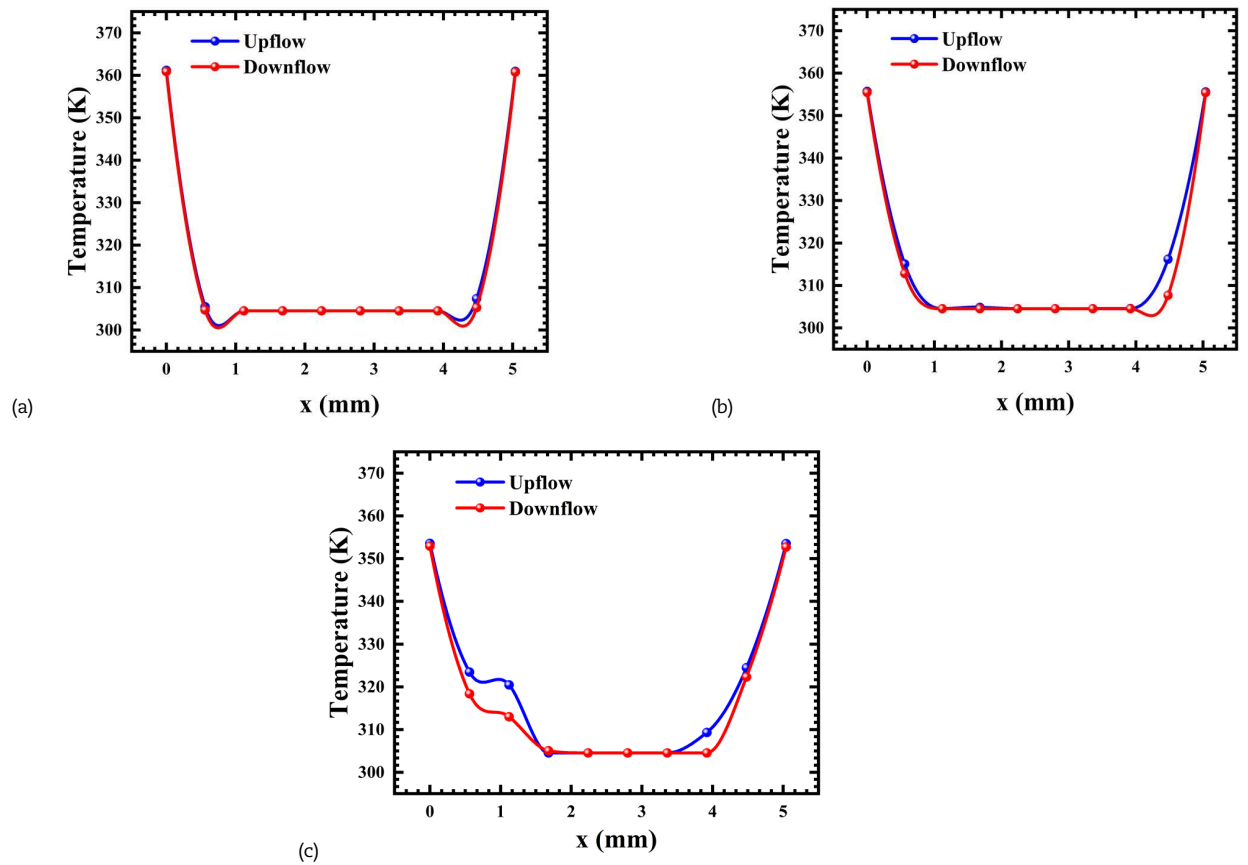


Fig. 7. Variation of fluid temperature within the minichannel in the vertical upflow and downflow orientations for different system pressures (a) $P = 102000$ Pa, (b) $P = 120000$ Pa, and (c) $P = 209000$ Pa.

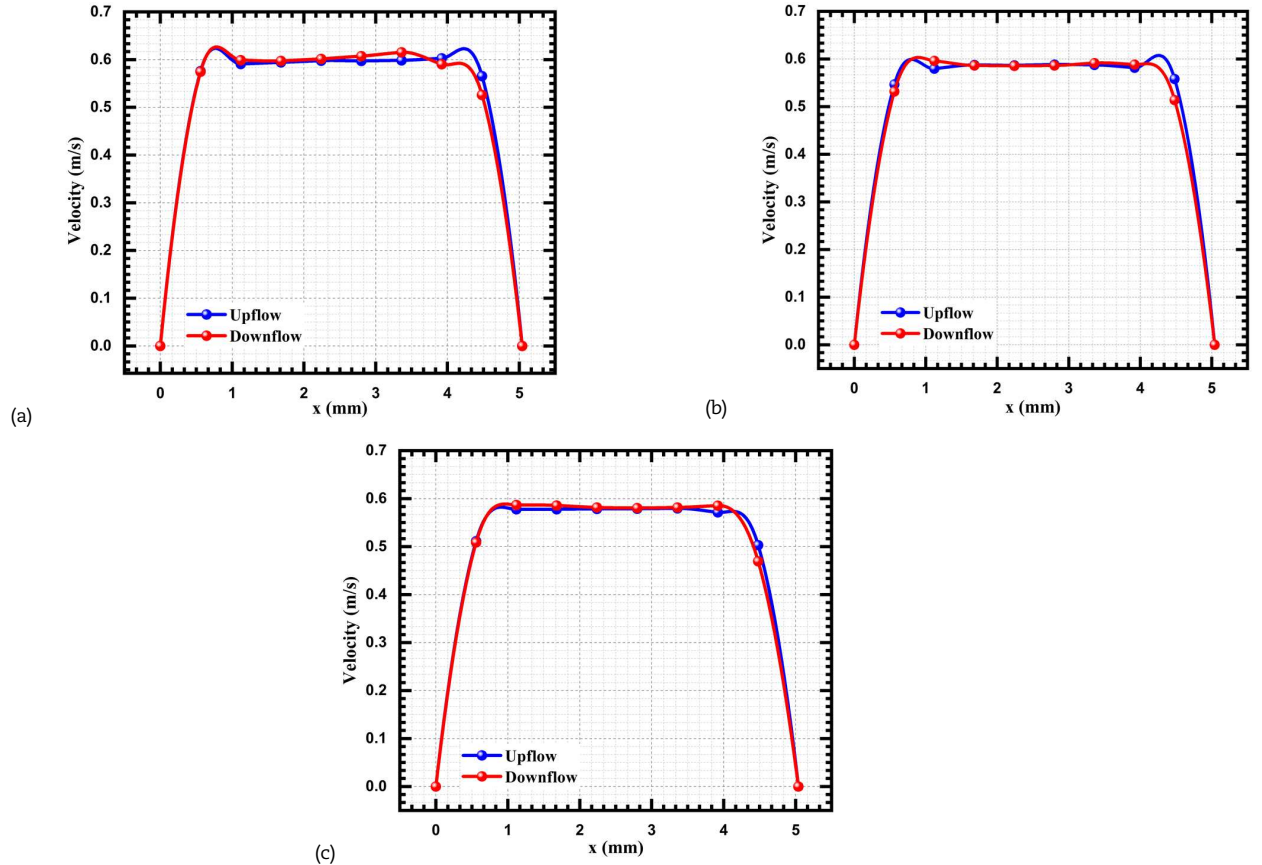


Fig. 8. Variation of velocity within the minichannel in the vertical upflow and downflow orientations for different system pressures (a) $P = 102000$ Pa, (b) $P = 120000$ Pa, and (c) $P = 209000$ Pa.



According to Fig. 6, it can be observed that for all system pressures, the orientation has a considerable effect on the heat transfer. The highest values of the heat transfer coefficient are obtained in the vertical upflow minichannel. An average improvement of 1.65% in the heat transfer is achieved in the upflow orientation for a system pressure of 209900 Pa. That is because, in the vertical upflow orientation, the fluid flow occurs in a fluent manner supported by the buoyancy force that moves the bubbles towards the flow direction and leads to fewer chaotic liquid-vapor interactions. In addition, Fig. 7 reveals that, for higher system pressure, the fluid temperature is much higher in the vertical upflow direction than in the downflow one, but in low system pressure, the effects of orientation on the fluid temperature are negligible and are nearly unchanged.

On the other hand, in the case of vertical downflow orientation, the buoyancy force is reduced by the rapidly moving fluid, as is demonstrated in Fig. 8 of flow velocity variation as a function of special orientation for different system pressures. From this figure, we can see that the flow velocity in the downflow orientation is slightly higher than in the upflow one, which causes stronger interactions between flow inertia and vapor buoyancy. This means the interactions between the accelerating flowing liquid and vapor bubbles that are still attached to the walls due to the opposing buoyancy force. Therefore, the heat transfer decreased. Furthermore, Fig. 9 shows that the flow velocity increases with a rise in the system pressure.

Figure 6 also demonstrates that the system pressure has a highly significant effect on the heat transfer coefficient. This figure shows that in the vertical upflow orientation, the increase in system pressure from 102000 Pa to 209900 Pa allows for enhancing the heat transfer coefficient by an average enhancement of 15.94%, which is associated with the variation of the fluid properties. The increase in pressure induces an increase in the thermo-physical properties of the liquid and vapor phases, as shown in Table 1, which promotes the activation of many nucleation sites and, therefore, improves heat transfer.

Figure 10 proves that the orientation has a significant effect on the vapor fraction. For all system pressures, the highest values of vapor fraction are achieved in the vertical upflow orientation due to the relatively small fluid velocity, which allows for an extended wall-fluid contact time. Therefore, the development of a large number of nucleation sites in the vertical upflow as compared to the vertical downflow orientation. This figure also indicates that the vapor fraction increases as the system pressure rises as a result of the increase in the densities of the liquid and vapor phases, thus supporting the activation of numerous nucleation sites.

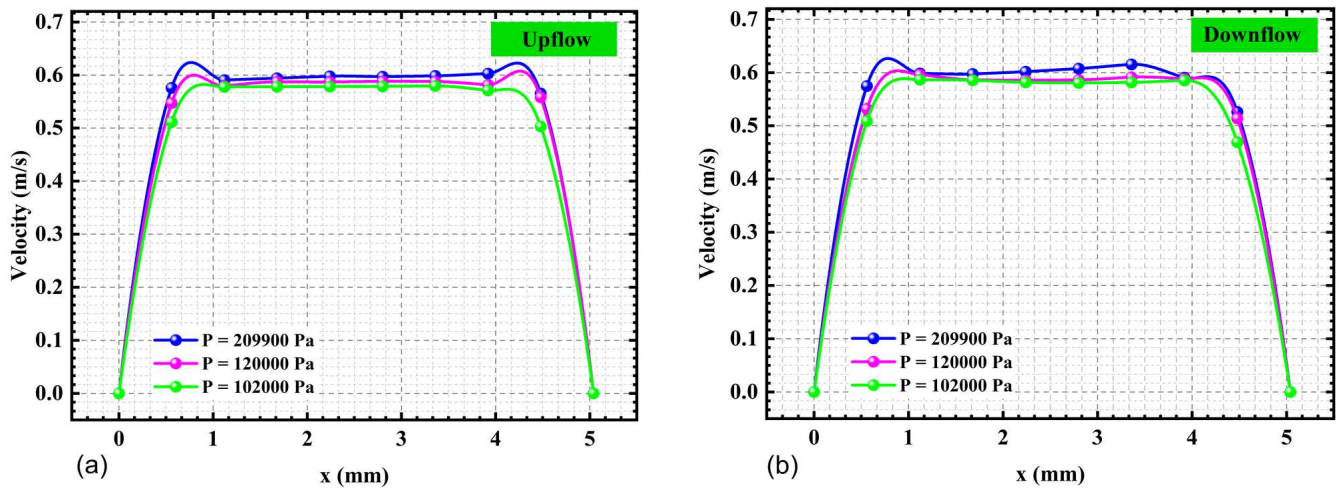


Fig. 9. Variation of velocity within the minichannel for different system pressures in (a) vertical upflow and (b) vertical downflow orientations.

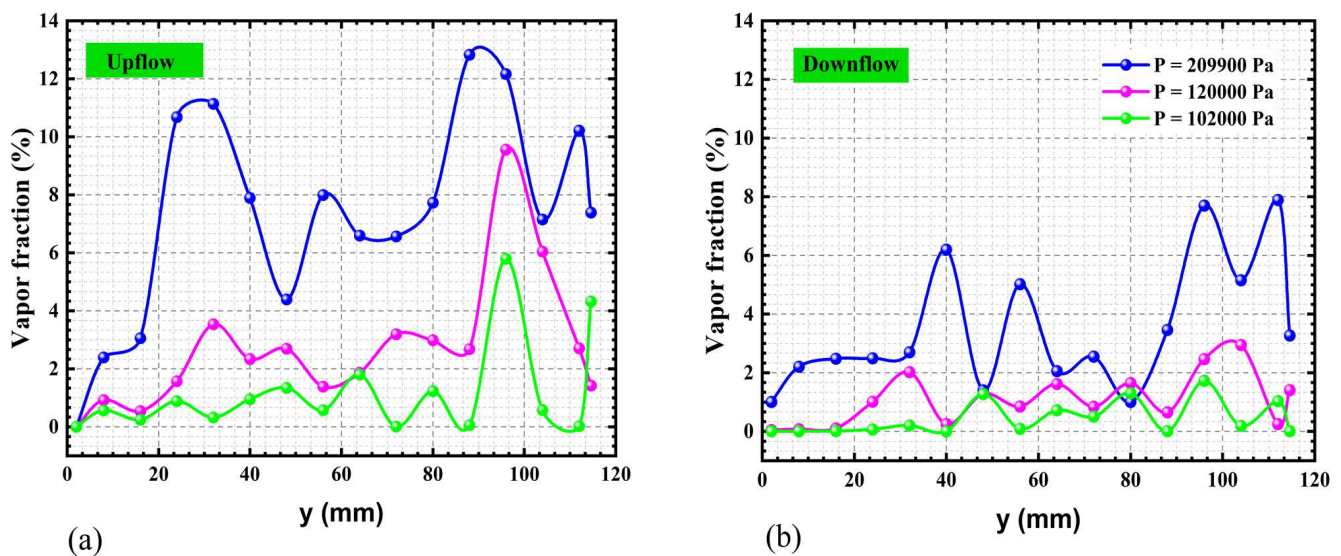


Fig. 10. Variation of time-averaged vapor fraction within the minichannel for different system pressure in (a) vertical upflow orientation and (b) vertical downflow orientation.



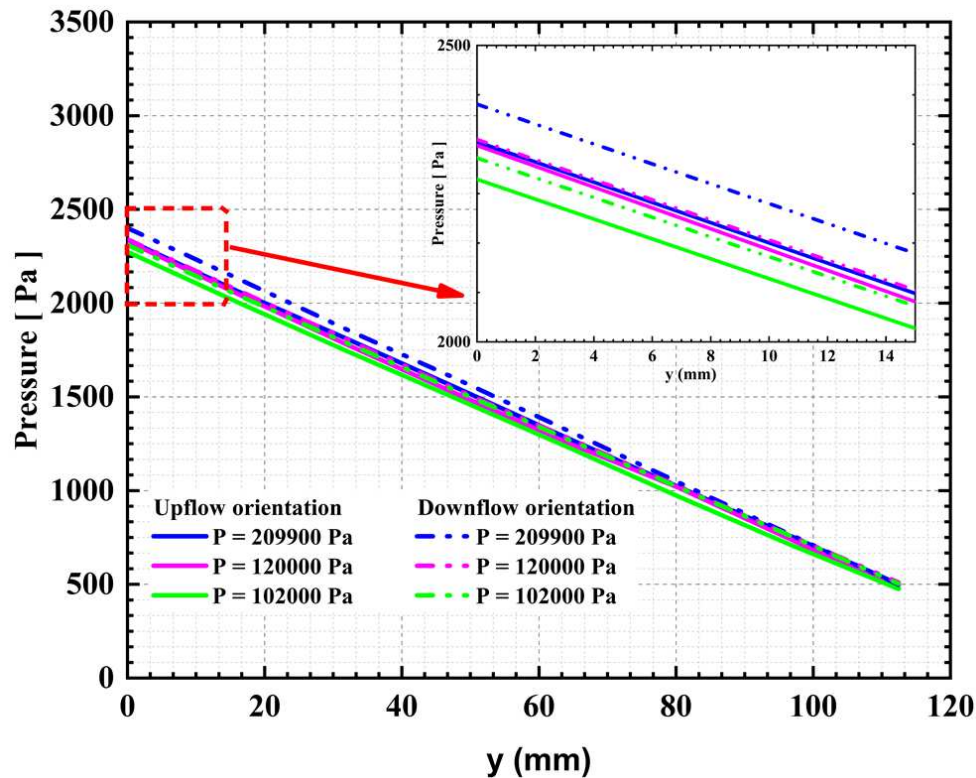


Fig. 11. Pressure drop variation in vertical upflow and downflow orientations for different system pressures.

The effect of orientation on the pressure drop along the minichannel for different system pressures is presented in Fig. 11. This figure shows that the vertical upflow position has less pressure drop, with an average enhancement of 3.25% for $P = 209900$ Pa due to the relatively small flow velocity in this orientation compared to the vertical downflow orientation. Furthermore, Fig. 11 shows that the pressure drop rises with increasing system pressure due to the increase in the thermo-physical properties of the liquid and vapor phases.

5. Conclusion

This work presented the computational results of subcooled flow boiling in a minichannel in two different orientations: vertical downflow and vertical upflow for different system pressures ($P = 102000$, 120000 , and 209900 Pa). The major conclusions of this study are as follows:

- The validation test of the present numerical results has demonstrated that they are in good agreement with the experimental data. The average relative errors have registered values of 18.097% and 20.687% for the left and right walls, respectively, which proves the efficiency of the current numerical model.
- The increase in the system pressure improves the heat transfer by improves the heat transfer by 15.94% from 102000 Pa to 209900 Pa.
- The vertical upflow orientation improves the heat transfer by 1.65% for the system pressure of 209900 Pa, whereas the vertical downflow position leads to the creation of severe reflux characteristics.
- The vertical upflow orientation decreases the pressure drop by 3.24% for a system pressure of 209900 Pa.

Author Contributions

A. Igaadi carried out and developed the numerical model, simulations, validation, data curation and prepared the original manuscript; H. El Mghari examined and edited the manuscript; R. El Amraoui supervised the work.

Acknowledgments

Not applicable.

Conflict of Interest

The authors declared no potential conflicts of interest concerning the research, authorship, and publication of this article.

Funding

The authors received no financial support for the research, authorship, and publication of this article.

Data Availability Statements

The datasets generated and/or analyzed during the current study are available from the corresponding author on reasonable request.



Nomenclature


E	Energy	Greek symbols	
F_{csf}	Surface tension force [N]	α	Volume fraction
g	Gravity acceleration [m/s^2]	β	Time relaxation fact [s^{-1}]
G	Mass flux [kg/m^2s]	λ	Conductivity [$W/m K$]
h	Heat transfer coefficient [W/m^2K]	ρ	Density [kg/m^3]
h_{lv}	Specific latent heat [J/kg]	μ	Dynamic viscosity [$Pa.s$]
k	Turbulent kinetic energy [J/kg]	σ	Surface tension coefficient [N/m^2]
q	Heat flux [W/m^2]	k	Local interface curvature
u	Flow velocity [m/s]	Subscript	
u_t	Friction velocity [m/s]	eff	Effective
P	Pressure [Pa]	in	Inlet
S	Source term	l	Liquid phase
t	Time [s]	lv	Liquid vapor mixture
Δt	Time step	sat	Saturation temperature
T	Temperature [K]	v	Vapor phase
		w	Wall

References

- [1] Belyaev, A.V., Varava, A.N., Dedov, A.V., Komov, A.T., An experimental study of flow boiling in minichannels at high reduced pressure, *International Journal of Heat and Mass Transfer*, 110, 2017, 360-373.
- [2] Celata, G.P., Cumo, M., Mariani, A., Experimental evaluation of the onset of subcooled flow boiling at high liquid velocity and subcooling, *International Journal of Heat and Mass Transfer*, 40(12), 1997, 2879-2885.
- [3] Martín-Callizo, C., Palm, B., Owhaib, W., Subcooled flow boiling of R-134a in vertical channels of small diameter, *International Journal of Multiphase Flow*, 33(8), 2017, 822-832.
- [4] Liu, Z., Bi, Q., Guo, Y., Su, Q., Heat transfer characteristics during subcooled flow boiling of a kerosene kind hydrocarbon fuel in a 1mm diameter channel, *International Journal of Heat and Mass Transfer*, 55(19-20), 2012, 4987-4995.
- [5] Nedaei, M., Motezakker, A.R., Zeybek, M.C., Sezen, M., Ince, G.O., Kosar, A., Subcooled flow boiling heat transfer enhancement using polyperfluorodecylacrylate (pPFDA) coated microtubes with different coating thicknesses, *Experimental Thermal and Fluid Science*, 86, 2017, 130-140.
- [6] Şişman, Y., Sadaghiani, A.K., Khedir, K.R., Brozak, M., Karabacak, T., Koşar, A., Subcooled Flow Boiling Over Microstructured Plates in Rectangular Minichannels, *Nanoscale and Microscale Thermophysical Engineering*, 20(3-4), 2016, 173-190.
- [7] Jiayao, L., Jinping, L., Rixin, L., Xiongwen, X., Experimental study on flow boiling characteristics in a high aspect ratio vertical rectangular mini-channel under low heat and mass flux, *Experimental Thermal and Fluid Science*, 98, 2018, 146-157.
- [8] Zahid, A., Björn, P., Rahmatollah, K., Flow boiling heat transfer and dryout characteristics of R152a in a vertical mini-channel, *Experimental Thermal and Fluid Science*, 53, 2014, 207-217.
- [9] Belyaev, A.V., Varava, A.N., Dedov, A.V., Komov, A.T., Critical heat flux at flow boiling of refrigerants in minichannels at high reduced pressure, *International Journal of Heat and Mass Transfer*, 122, 2018, 732-739.
- [10] Charnay, R., Revellin, R., Bonjour, J., Flow boiling characteristics of R-245fa in a minichannel at medium saturation temperatures, *Experimental Thermal and Fluid Science*, 59, 2014, 184-194.
- [11] Yan, Q., Jia, L., An, Z., Peng, Q., A comprehensive criterion for slug-annular flow transition based on flow boiling of R134a in microchannels, *International Communications in Heat and Mass Transfer*, 105, 2019, 1-9.
- [12] Chen, S., Chen, X., Luo, G., Zhu, K., Chen, L., Hou, Y., Flow boiling instability of liquid nitrogen in horizontal mini channels, *Applied Thermal Engineering*, 144, 2018, 812-824.
- [13] Brutin, D., Tadrist, L., Pressure drop and heat transfer analysis of flow boiling in a minichannel: influence of the inlet condition on two-phase flow stability, *International Journal of Heat and Mass Transfer*, 47(10-11), 2001, 2365-2377.
- [14] Piasecka, M., Maciejewska, B., Heat transfer coefficient during flow boiling in a minichannel at variable spatial orientation, *Experimental Thermal and Fluid Science*, 68, 2015, 459-467.
- [15] Vlachou, M.C., Karapantsios, T.D., Effect of channel inclination on heat transfer and bubble dynamics during subcooled flow boiling, *International Journal of Thermal Sciences*, 124, 2018, 484-495.
- [16] Piasecka, A., Strąk, K., Maciejewska, B., Heat transfer characteristics during flow along horizontal and vertical minichannels, *International Journal of Multiphase Flow*, 137, 2021, 103559.
- [17] Sinha, G.K., Srivastava, A., Experiments to compare the dynamics and thermal impact of single vapor bubble subjected to upward and downward flow boiling configurations, *Experimental Heat Transfer*, 33(6), 2020, 487-509.
- [18] Vermaak, M., Orejon, D., Dirker, J., Sefiane, K., Meyer, J.P., Pressure and Thermal Characterisation of Dynamic instabilities during Flow Boiling in Micro/Mini-Channels at Different Azimuth Orientations, *Applied Thermal Engineering*, 218, 2022, 119292.
- [19] Vermaak, M., Potgieter, J., Dirker, J., Moghimi, M.A., Valluri, P., Sefiane, K., Meyer, J.P., Experimental and Numerical Investigation of Micro/Mini Channel Flow-Boiling Heat Transfer with Non-Uniform Circumferential Heat Fluxes at Different Rotational Orientations, *International Journal of Heat and Mass Transfer*, 158, 2020, 119948.
- [20] Brackbill, J.U., Kothe, D., Zemach, C., A continuum method for modeling surface tension, *Journal of Computational Physics*, 100, 1992, 130-139.
- [21] Lee, W.H., A pressure iteration scheme for two-phase flow modeling, Verizoglu, T.N. (ed.), *Multiphase Transport Fundamentals, Reactor Safety, Applications*, Hemisphere Publishing, 1980.
- [22] Lee, J., O'Neill, L.E., Lee, S., Mudawar, I., Experimental and computational investigation on two-phase flow and heat transfer of highly subcooled flow boiling in vertical upflow, *International Journal of Heat and Mass Transfer*, 136, 2019, 1199-1216.

ORCID iD

Amal Igaadi  <https://orcid.org/0000-0002-0351-1362>

Hicham El Mghari  <https://orcid.org/0000-0001-5055-814X>





© 2022 Shahid Chamran University of Ahvaz, Ahvaz, Iran. This article is an open access article distributed under the terms and conditions of the Creative Commons Attribution-NonCommercial 4.0 International (CC BY-NC 4.0 license) (<http://creativecommons.org/licenses/by-nc/4.0/>).

How to cite this article: Igaadi A., El Mghari H., El Amraoui R. Numerical Investigation into the Effects of Orientation on Subcooled Flow Boiling Characteristics, *J. Appl. Comput. Mech.*, 9(2), 2023, 464–474.
<https://doi.org/10.22055/jacm.2022.41723.3802>

Publisher's Note Shahid Chamran University of Ahvaz remains neutral with regard to jurisdictional claims in published maps and institutional affiliations.

